FINITE ELEMENT MODELS OF PASSIVE CONTINENTAL MARGINS WITH IMPLICATIONS FOR THE INITIATION OF SUBDUCTION ZONES[1]

SIERD CLOETINGH[2] & RINUS WORTEL[2]

ABSTRACT

Cloetingh, S. & R. Wortel 1982 Finite element models of passive continental margins with implications for the initiation of subduction zones – Geol. Mijnbouw 61: 281-292.

Passive continental margins are in general characterized by the lateral contrast between oceanic and continental lithosphere and by the presence of thick sedimentary deposits which cause flexure and stressing of the lithosphere. Passive margins therefore, are potential sites for plate rupture and initiation of subduction.

To investigate the evolution of passive margins, we have constructed finite element models, in which we have incorporated a complex system of forces, depth-dependent rheological properties and lateral variations across the margin. Sediment loading generates differential stresses of several kilobars and dominates the state of stress at passive margins. Stresses of this order of magnitude may cause failure of the lithosphere and initiation of subduction. We have found that the aging of passive margins alone does not make them more susceptible to initiation of subduction.

However, extensive sediment loading on young lithosphere might be an effective mechanism for closure of small oceanic basins. This phenomenon plays an important role in the process of mountain building.

INTRODUCTION

The initiation of subduction is a key element in plate tectonic schemes for the evolution of the lithosphere. Nevertheless, up till the present time we have not understood very well the underlying mechanisms (e.g. DICKINSON & SEELY, 1979). Progress on this topic, recognized as an outstanding problem in earth sciences (KANAMORI, 1980), has lagged far behind advances made in the last few years in the analysis of other dynamical aspects of plate tectonics. The research presented here (see also CLOETINGH ET AL., 1981; 1982a, b) forms part of a systematic study of initiation of subduction.

Vlaar and Wortel (VLAAR, 1975; VLAAR & WORTEL, 1976; WORTEL, 1980) have shown that the age of the oceanic lithosphere (which controls its thermal and mechanical structure) is a fundamental parameter in the dynamics of plate motions. It was therefore decided to investigate whether age dependence of lithospheric properties might provide a clue to better understand the mechanism of initiation of subduction (CLOETINGH ET AL., 1981).

The lithosphere has considerable strength (KIRBY, 1980) and is capable of supporting differential stresses of the order of several kilobars on geological timescales (WATTS ET AL., 1980). Therefore, our study deals basically with an assessment of the possibilities for rupture of the lithosphere. In general, tectonic forces acting on the lithosphere (FORSYTH & UYEDA, 1975) do not generate stresses of several kilobars. Thus, special circumstances with a local concentration of forces, in an optimal combination with a suitable rheological structure, are required to induce lithospheric failure. It is therefore plausible that initiation of subduction takes place preferentially at pre-existing weakness zones or in regions where the lithosphere is stressed by forces arising from mechanisms not associated with these tectonic forces. Passive continental margins are characterized by a lateral contrast between oceanic and continental lithosphere and are commonly the sites of thick sedimentary deposits (WATKINS & DRAKE, 1982) which cause considerable flexure and stressing of the lithosphere. Reconstructions of sedimentary sequences incorporated in orogenic belts (STONELEY, 1969) yield estimates for maximum thicknesses comparable with those encountered at passive margins. These observations together with geological arguments put forward by others (DIETZ, 1963; DEWEY, 1969; SPEED & SLEEP, in prep.) make passive margins obvious

[1] Manuscript received: 1982-05-19.
Revised manuscript accepted: 1982-09-10.

[2] Dept of Theoretical Geophysics, Institute of Earth Sciences, University of Utrecht, Budapestlaan 3584 CD, Utrecht, The Netherlands.

potential sites for initiation of subduction. For a proper assessment, however, a model study is essential. Model studies of the evolution of passive margins are of increasing importance for the evaluation of their petroleum potential (EMERY, 1980; WATKINS & DRAKE, 1982).

The state of stress at passive continental margins is a complicated subject as it is determined by local geometrical and rheological properties and by the system of forces acting on the lithosphere. The forces are the push exerted by the adjacent oceanic ridge (HALES, 1969), the negative buoyancy associated with the cooling of the oceanic lithosphere when it moves away from the spreading centre (VLAAR & WORTEL, 1976) and sediment loading at the margin (see further Fig. 3). Moreover, these properties and forces vary across the margin, making an analytical treatment inadequate. These considerations, in particular the possible implications of age-dependent properties of oceanic lithosphere, have not been taken into account in earlier work dealing with the state of stress at passive margins (WALCOTT, 1972; BOTT & DEAN, 1972; TURCOTTE ET AL., 1977). Finite element analysis provides a powerful tool to incorporate variable lithospheric properties and forces into passive margin models.

The present work is an example of an application of the finite element method on a level sufficiently advanced to cope with the complexity of geodynamic problems. The appendix to the article contains a short description of features of the finite element method pertinent to research in Geodynamics.

In our previous model studies (CLOETINGH ET AL., 1981; 1982a) we have shown that sediment loading dominates the state of stress at passive margins. In that work we have demonstrated that, owing to the continuing accumulation of sediments at passive margins, the stress level induced increases with the age of the margin. An important new feature following from more detailed rheological considerations to be discussed here, and implemented in the models, is that the strength of the lithosphere increases with age as well.

The results of our analysis provide insight into the conditions that govern the transition from passive margins into active margins. This applies in particular in the context of opening and closing of small oceanic basins.

STATE OF STRESS AT PASSIVE MARGINS

Sediment loading models

The sediment loading capacity of oceanic lithosphere increases with age, through its continued cooling and densification (which controls the subsidence of the ocean floor (PARSONS & SCLATER, 1977)). One might therefore expect a coupling of the thickness of the sedimentary sequence deposited at a passive margin with the age-dependent subsidence of the underlying lithosphere (TURCOTTE & AHERN, 1977). As a model for sedimentary loading we adopt two adjacent triangular sediment wedges at the continental shelf and the continental rise. As our reference we assume that the maximum thickness of the wedges corresponds with the thickness that can be expected if the sedimentation has been keeping up with the subsidence of a boundary layer model of the cooling oceanic lithosphere (TURCOTTE & AHERN, 1977; WORTEL, 1980). This implies that the maximum thickness of the sedimentary wedge will gradually increase and reach a maximum of 9.4 km at 200 m.y. (see Fig. 1), following roughly a square-root-of-age relation. In Fig. 1 we have plotted observational data on post-rift sedimentary thicknesess. From an inspection of Fig. 1 it follows that the *reference model* constitutes a fair average of the sediment loading histories and resulting thicknesses observed at passive margins.

The huge sediment accumulations found at deltas however, clearly exceed the thicknesses depicted by the reference model. Therefore, we adopt a second model of sedimentation, the *full load model,* in which the entire loading capacity of the oceanic lithosphere is taken up by sediments. In this model the maximum thickness of the sedimentary wedges reaches 16 km at 200 m.y. (see Fig. 1). As shown in Fig. 1 the sedimentary thicknesses of the full load model are characteristic for deltas. It should be noted that only deltas are listed which are at least partly deposited on oceanic lithosphere. The Nile cone (thickness at least 8 km, MALOVITSKYI ET AL., 1975) and the Po fan (thickness of the order of 7 km, FINETTI & MORELLI, 1973) have considerable thicknesses, but they are deposited on (thinned) continental crust of the eastern Mediterranean (CLOETINGH ET al., 1980a) and Adriatic Sea (NOLET ET AL., 1978) respectively, and therefore excluded from Fig. 1.

The width of the sedimentary wedges is on the average 250 km, although for young margins widths as small as 150 km are found (e.g. some western Mediterranean basins, see also WATKINS & DRAKE, 1982). As the sediments on the margin replace water, we consider only the excess density $\Delta\varrho = \varrho$ (sediment) $- \varrho$ (seawater) $= 1.4$ g cm^{-3}.

Rheology of the oceanic lithosphere

The flexure of oceanic lithosphere has been studiled where it bends at oceanic trenches (CHAPPLE & FORSYTH, 1979; MCADOO ET AL., 1978) and under the influence of seamount loading (WATTS ET AL., 1980). These analyses have demonstrated that the lithosphere is capable of supporting stresses of the order of several kilobars on geological timescales. The thermally defined lithosphere has its lower boundary at a depth, approximately corresponding with the 1200°C isotherm. We define the depth at which the strength is 500 bar as the lower boundary of the *mechanically strong upper part of the lithosphere.* Thermal models for the oceanic lithosphere (CROUGH, 1975; PARSONS & SCLATER, 1977) indicate that the base of this part of the lithosphere coincides with an isotherm of about 600–700°C. Once a lithosphere plate is loaded, rapid

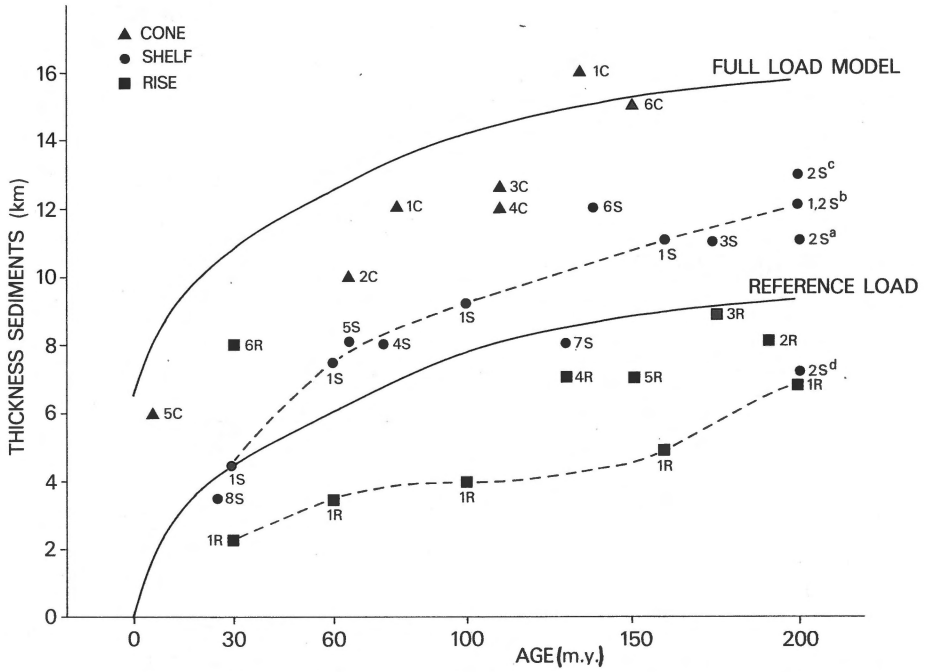

Fig. 1

The increase of sediment thickness versus age adopted for the reference load and full load models (solid curves) compared with data on post-rift sedimentary thicknesses at passive continental margins. Symbols ●, ■ and ▲ denote maximum thicknesses of post-rift shelf, rise and fan deposits respectively. Data are taken from the following sources:

● 1S Eastern U.S. shelf off New Jersey based on the cost-B2 well Dashed curve gives the sediment loading history (Grow et al., 1979). 2S Carolina through (2a), Blake plateau (2b), Baltimore canyon (2c), and Georges Bank (2d) (Grow & Sheridan, 1981). 3S Nova Scotia shelf (Keen, 1979). 4s Labrador shelf (Hinz et al., 1979). 5S Western Indian shelf (Closs et al., 1974). 6S Shelf off Kenya (Kent, 1974). 7S South Argentina shelf (Urien et al., 1976). 8 S Gulf of Lyon (Watts & Ryan, 1976).

■ 1R Eastern U.S. continental rise off New Jersey based on the Cost-B2 well. Dashed curve gives the sediment loading history (Grow et al., 1979). 2R Morocco rise (Goldflam et al., 1980). 3R Nova Scotia rise (Watts & Steckler, 1979). 4R South Argentina rise (Urien et al., 1976). 5R Gulf of Mexico rise (Buffer et al., 1981). 6R Baffin Bay (Keen & Keen, 1974)

▲ 1C Bengal fan (Curray and Moore, 1974). 2C Indus Cone (Naini, 1980). 3C Niger Cone (Lehner & De Ruiter, 1977). 4C Amazon cone (Houtz et al., 1977; Cloetingh et al., 1979, 1980b). 5C Colorado fan (Crowell, 1974). 6C Mississippi fan (Buffler et al., 1981).

stress relaxation takes place in its lower part (MINSTER & ANDERSON, 1980), and stresses are concentrated in its upper part. Thus modelling the lithosphere as a layer with an uniform elastic upper part and a plastic lower part (with a relatively low yield strength) provides a good first order description of the mechanical properties of the lithosphere (CALDWELL & TURCOTTE, 1979) and was adopted in our previous models (CLOETINGH ET AL., 1981, 1982a).

More information on the depth-dependence of the rheological properties of the lithosphere has become available through the experimental work by Goetze and coworkers (GOETZE, 1978; GOETZE & EVANS, 1979) on deformation of olivine, the mineral which is the dominant constituent of oceanic lithosphere, and through studies of the flexural behaviour of oceanic lithosphere (BODINE ET AL., 1981).

These investigations show that three deformation zones are present in bending of the lithosphere. At the top the deformation is in the brittle regime and the (Coulomb) strength increases strongly with pressure. The deformation is not sensitive to variations in temperature and strain-rate, and the strength does not depend on rock type. Near the central plane of the bending lithosphere, stresses are supported by the elastic core of the plate.

In the lower part of the plate the effects of temperature become dominant and stresses are limited by ductile flow. The ductile deformation is relatively pressure insensitive, but is very sensitive to temperature, to differential stress and to a far lesser extent to strain-rate.

At high stresses dislocation glide is the dominant creep process. The ductile flow is described by the Dorn-creep equation (GOETZE, 1978), which holds for stresses above 2 kilobar:

$$\dot{e} = \dot{e}_1 \exp\{-[Q_1(1-\sigma/\sigma_p)^2/RT]\}$$

where $\dot{e}$ is the strain-rate (s^{-1}), σ is the differential stress, Q the activation energy (Q_1 = 128 kcal/mole) for dry olivine, R is the universal gas constant and T is the temperature (K). $\dot{e}_1 = 5.7 \times 10^{11} s^{-1}$ and σ_p = 85 kbar are constants.

At stresses below 2 kilobar creep by thermally activated climb of dislocations becomes effective. This process is described by a power-law creep equation (GOETZE, 1978):

$$\dot{e} = \dot{e}_2 \sigma^3 \exp[-Q_2/RT],$$

with Q_2 = 122 kcal/mole and, for σ in bars, $\dot{e}_2$ = 70 $bar^{-3}s^{-1}$.

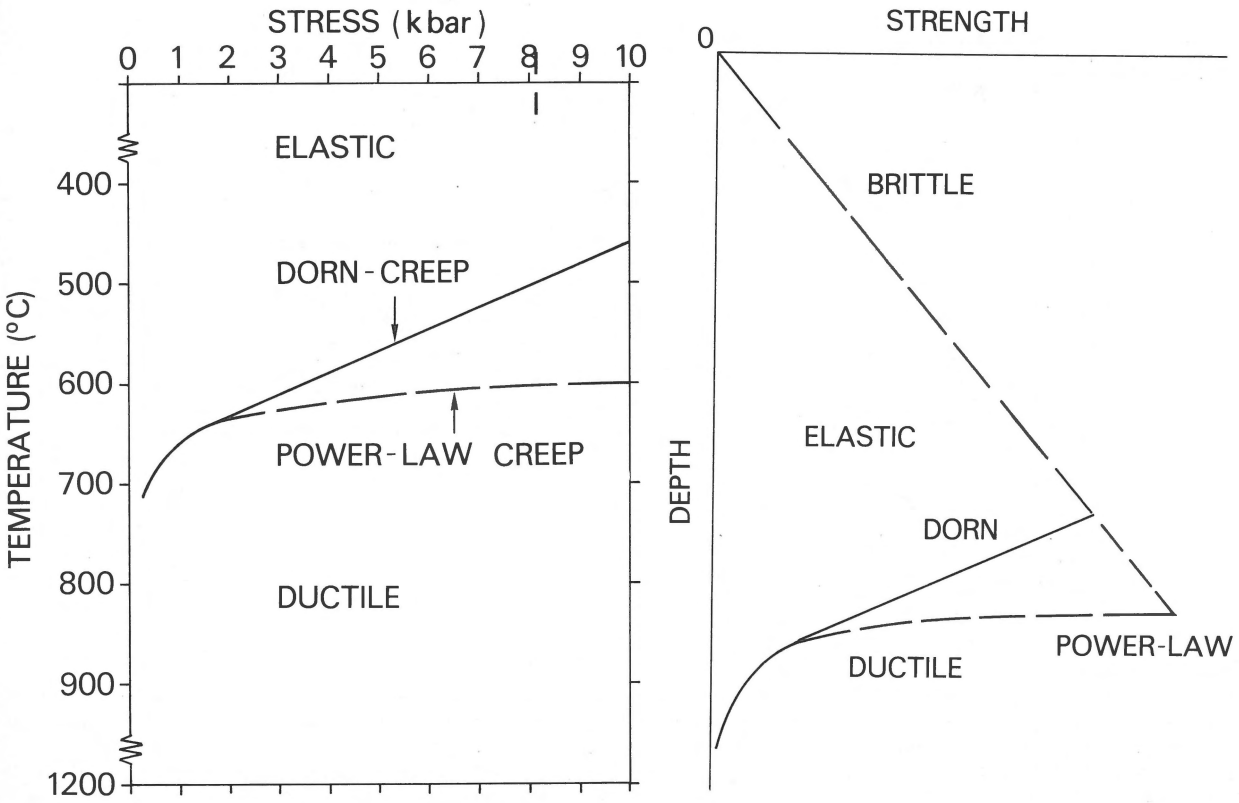

Fig. 2.
Rheological model for the oceanic lithosphere based on olivine rheology. Three regions are present in the mechanically strong part of the lithosphere: The top is characterized by brittle fracture, the central core is in the elastic regime and the lower part is deforming according to ductile flow. After Goetze (1978) power-law creep and Dorn-creep, dominant at stresses below and above 2 kbar respectively, determine the transition between the elastic and ductile regime.
a (left). The transition stress between the elastic regime and the region dominated by ductile flow (solid curve). The lower boundary of the lithosphere is defined by a temperature of 1200°C.
b (right). The strength profile through the upper part of the lithosphere derived from Fig. 2a by specifying the temperature function inside the lithosphere according to Crough's (1975) thermal model. (See Fig. 5 for specific shapes of the strength envelopes for different ages of the oceanic lithosphere). At shallow depths pressure effects on the strength dominate and deformation is in the brittle regime, indicated by the dashed line.

A strength profile for the lithosphere can now be constructed by combining the constitutive equations for the brittle, elastic and ductile regimes (Fig. 2a). Once the temperature profile and the brittle and ductile behaviour are specified, the transition from the eleastic to a ductile state is completely determined for a given strain-rate (Fig. 2b). For specific shapes of the strength envelopes for different ages of the oceanic lithosphere the reader is referred to Fig. 5.

The increase in strength with depth inside the sedimentary section at the top of the lithosphere is usually linear as stated by BRYANT ET AL. (1981). These authors observe that, presumably due to porosity contrasts, the shear strength-depth profile is a function of sediment type and age. They point out also that, even amongst seemingly similar sediment types, a considerable range of shear strengths versus depth has been measured at shallow levels. Further down large uncertainties in strength arise. Therefore, instead of making an uncertain estimate, we attribute a zero strength to the sediments. Numerical experiments have shown us that the effect of variations in strength in the top ten kilometres of the plate has a very modest effect on the stress distribution within the plate as a whole.

We have derived strenght envelopes from Goetze's flow laws for olivine, with an assumed strain-rate of $\dot{e} = 10^{-18}s^{-1}$ (characteristic for sedimentary basin development) for oceanic lithosphere of ages up to 200 m.y. Temperature profiles are based on CROUGH'S (1975) model for the oceanic lithosphere, which combines the merits of the boundary layer model (TURCOTTE & OXBURGH, 1967) and the plate model (MCKENZIE, 1967; PARSONS & SCLATER, 1977; see WORTEL, 1980, for a review). A similar approach was followed by BODINE ET AL. (1981). The thickness of the mechanically strong part of the lithosphere and its maximum strength are strongly dependent on age. Both increase according to a square-root-of-age function from a few kilometers, respectively a few kilobars for young lithosphere to values of

approximately 50 km and 10 kbar for old oceanic lithosphere (see also Figs. 3 and 5). The effect of variations in strain-rate is much less pronounced; an order of magnitude variation in strain-rate corresponds to only a 1-2 km change in the thickness of the mechanically strong part of the lithosphere.

MODEL CALCULATIONS AND RESULTS

Description of the finite element models

We have constructed finite element models for a passive continental margin in different stages of evolution, at ages of 20, 30, 60, 100 and 200 m.y. respectively. For all models a half-spreading rate of 1 cm/yr. is taken, characteristic for oceanic lithosphere without attached downgoing slabs (FORSYTH & UYEDA, 1975). The calculations were carried out with the MARC finite element package (MARC, 1980). The model features are summarized in Fig. 3. Age-dependent lithospheric thicknesses are based on CROUGH's (1975) model for the oceanic lithosphere. A thickness of 150 km inferred from a number of independent geophysical approaches (e.g. POLLACK & CHAPMAN, 1977) is assigned to the continental lithosphere.

We adopt a width of 200 km for the transition between oceanic and continental lithosphere, taking into account the evidence for the presence of rift-stage crust at the margin (HUTCHINSON ET AL., 1982). The depth dependent rheology of the oceanic lithosphere is based on Fig. 2. A thickness of 60 km for the mechanically strong upper part of the adjacent continental lithosphere is based on HAXBY ET al. (1976). Rheological profiles under the shelf and in the rift-stage crust have been constructed by linear interpolation between the rheologies of the adjacent oceanic and continental lithospheres. This approach is supported by the results of temperature calculations by ZIELINSKI (1979), showing a gradual and linear 100-300 km wide transition in the temperature profiles across the margin, from ocean towards the continent. This concerns in particular the isotherms for temperatures below 600-700°C which are most pertinent to the mechanical properties at the margin. Eventual weakness zones associated with the break-up stage of passive margins possibly influence the state of stress, in particular in the early post-rift phase. However, recent modelling of subsidence at passive margins (STECKLER & WATTS, 1981) has provided strong evidence that faults associated with the break-up phase are locked early in their post-rift evolution. Therefore, we refrain from incorporating mechanical weakness zones and discontinuities (fossil fault zones) in our models.

The two models for sediment loading at the margin have been discussed in the previous section. The resulting flexure of the lithosphere is counteracted by isostasy. Isostatic forces proportional to the deflection due to loading are included in the models. Of the plate tectonic forces which are implemented in the models, the magnitudes of the forces associated with the ridge push and the negative buoyancy of the oceanic lithosphere are calculated on the basis of OXBURGH & PARMENTIER's (1977) model for the formation of oceanic crust and CROUGH's (1975) model for the thermal evolution of oceanic lithosphere. The ridge push is often modelled as a line force. Physically it is more appropriate to consider it as a force resulting from a horizontal pressure gradient due to density variations. The integrated pressure gradient per unit width along the ridge, for oceanic lithosphere with an age of 100 m.y., is 2.3×10^{12} N/m. We neglect drag at the base of the lithosphere. Zero horizontal displacements are prescribed for the right hand boundary of the model to simulate a ridge push transmitted through the continent from an adjacent oceanic plate.

The accuracy of the finite element calculations was checked and confirmed by convergence tests and an analysis of the internal reaction forces of the model. For further details on the numerical aspects of the work the reader is referred to the Appendix (see also CLOETINGH & WISSE, 1981).

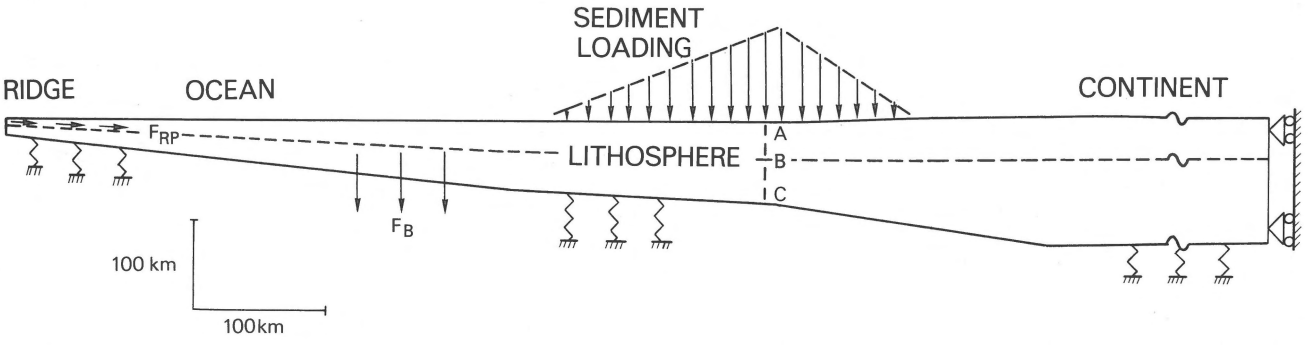

Fig. 3
Model features: geometry, rheology, system of forces and boundary conditions. The bottom of the mechanically strong part of the lithosphere is indicated by a broken horizontal line. Young's modules $E = 7 \times 10^{10} N/m^2$ and Poisson's ratio $\nu = 0.25$. F_{RP} is the push exerted by the oceanic ridge, F_B is the negative buoyancy associated with the cooling of the oceanic lithosphere when it moves away from the spreading centre. Isostatic forces counteracting the deflection are indicated by springs.

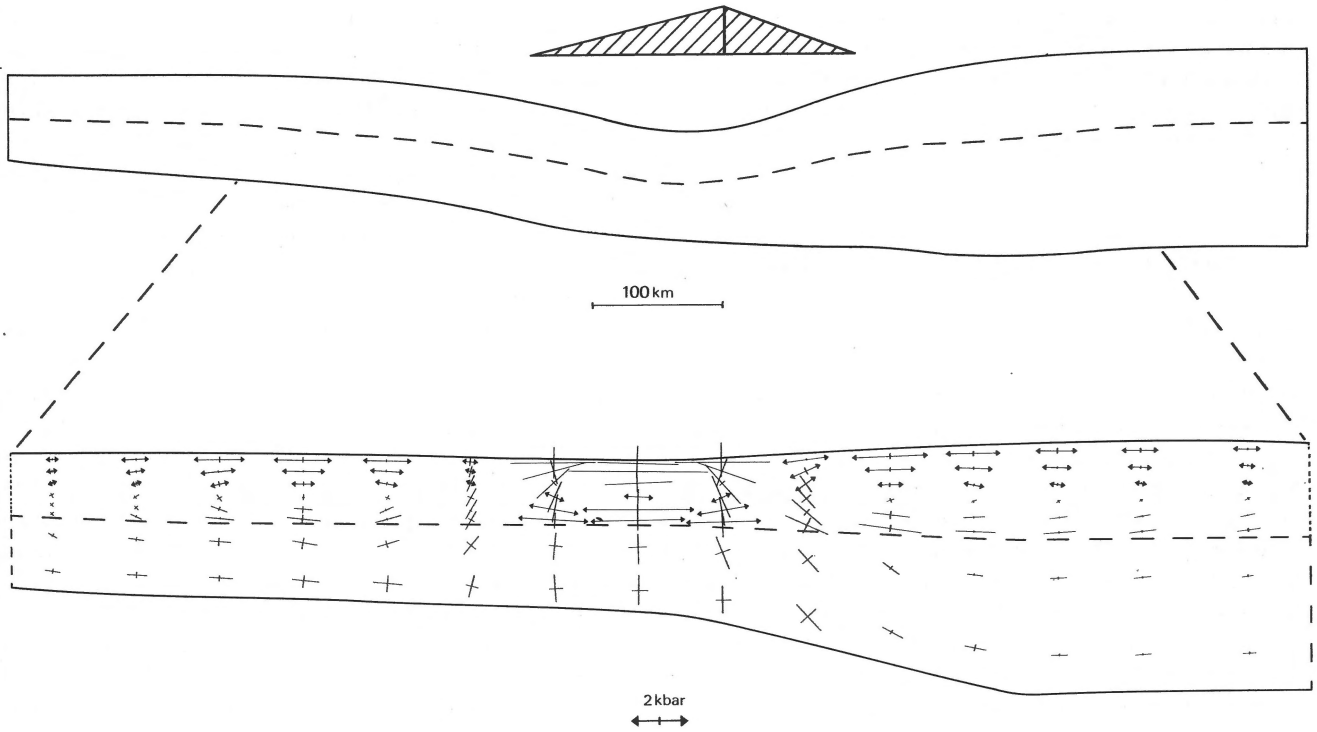

Fig. 4
Deflection and stresses calculated for a passive margin with an age of 100 m.y., based on the reference model of sediment loading, given in Fig. 1. Flexure caused by sediment loading forms the dominant deformation mode at the margin. Principal stresses denoted by arrows are plotted in the undeformed configuration. Stresses and displacements are plotted only for the parts of the lithosphere were the deformation is significant.
a (above), Displacement of the lithosphere (km). Note that the scale of the the displacement (vertical axis) and geometry (indicated by a horizontal bar at the bottom of the figure) are not the same.
b (below), Principal stresses (kbar) at the margin. Symbols (⟷) and (—|—) denote tension and compression respectively.

Results

In Fig. 4 the results of the model calculations are displayed for a passive margin with an age of 100 m.y., with sediment loading according to the reference model. The deformation of the lithosphere and the resulting stress field (order of magnitude a few kbar) is dominated by the sediment loading; the contribution of the plate tectonic forces to the stress field is an order of magnitude smaller.

Differential stresses are largest at the points of maximum flexure. The largest stress maximum is located under the continental rise in oceanic lithosphere close to the transition of oceanic and rift-stage lithosphere. In Figs. 5a and 5b the stress maxima for 100 m.y. and 30 m.y. are displayed for the reference load, as a function of depth, down to the base of the mechanically strong upper part of the lithosphere. Hatched areas indicate failure by brittle fracture in the uppermost part and by ductile flow in the lowermost part of the mechanically strong part of the lithosphere, respectively. Its main part is in the elastic state. If the full loading capacity of the lithosphere is taken up by sediments, this can even result in complete failure of the lithosphere as demonstrated in Fig. 5c.

Fig. 5 also shows that the state of stress is dependent on the age of the margin. To illustrate this dependence more clearly we have plotted in Fig. 6a the maximum differential (tensional) stresses as a function of age for the reference load. The age-dependence is strongest for ages below 100 m.y..

From 30 to 100 m.y. – an interval in which the sedimentary loading, the thickness of the mechanically strong part of the lithosphere, and the strength increase – the differential stress maxima are found to increase strongly with age. From 100 to 200 m.y. the thickness of the mechanically strong part of the lithosphere and its strength show only a small increase. For ages above 100 m.y. the increase in sediment loading according to our reference model results only in a minor increase of the stresses.

Interesting quantities are the ratio of the maximum stress generated and the maximum strength, the relative thickness of the mechanically strong upper part in failure H_y/H and the ratio of A_y, corresponding with the hatched area inside the strength envelope (Fig. 5), and the total area A of the envelope. For the reference model of sediment loading these quantities prove to be essentially independent of age.

The situation is drastically different if the full loading capacity is taken up. The surplus load of sediments added to the reference load is most effective in creating high stresses when deposited on a young margin. Of the three ratios plotted in Fig. 6a we select the ratio A_y/A as the most meaningful

quantity to illustrate the evolution of the stress pattern for full loading conditions. Quantity A (or A_y) is a combined measure of the thickness and strength of the mechanically strong upper part of the lithosphere. The ratio A_y/A as plotted in Fig. 6b as a function of the age of the margin. Fig. 6b and results of numerical calculations made for ages below 20 m.y. (not shown here) demonstrate that full loading on a young passive margin (age below 20 m.y.) leads to complete failure of the lithosphere.

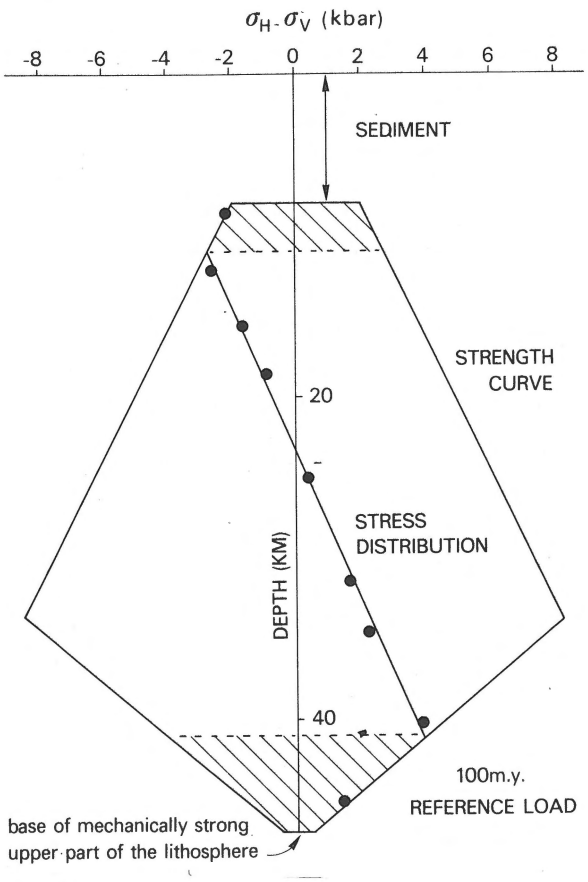

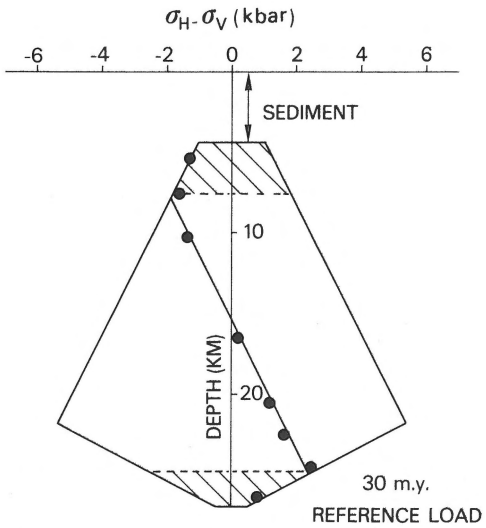

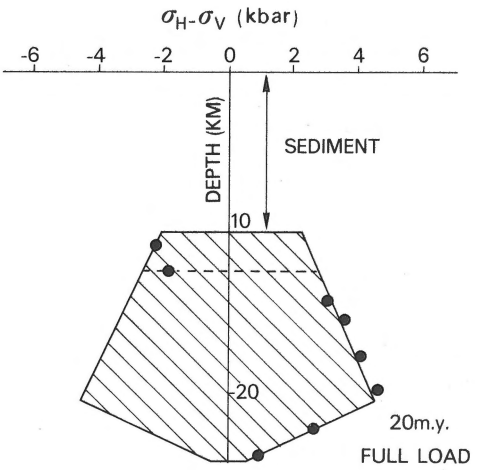

Fig. 5
Comparison of stresses generated at the margin with lithospheric strength. Strength envelope and results of stress calculations (solid dots) as a function of depth down to the base of the mechanically strong upper part of the lithosphere at the point of maximum flexure (AB of cross section ABC in Fig. 3; see also Fig. 4). The line inside the strength envelope connecting the solid dots is the stress distribution. Differential stresses ($\sigma_H - \sigma_V$) are plotted versus depth. Sign convention for the stresses: tension positive, compression negative. Zero-strength has been assumed for the sediments. Hatched areas in the upper and lower part of the mechanically strong upper part of the lithosphere denote failure by brittle fracture and ductile flow respectively. *a* (left), *b* (upper right), the results for the reference model of sediment loading for ages of 100 and 30 m.y. *c.* (lower right), the results for the full load model for 20 m.y. The horizontal dashed line indicates the neutral surface just before complete failure of 20 m.y. old lithosphere takes place.

DISCUSSION

The results of our model calculations show that sediment loading at a passive margin can induce flexural stresses of several kilobars. Considering this order of magnitude, it is justified to neglect here (see also CLOETINGH ET AL., 1981; 1982a, b) relatively minor effects of stresses due to crustal thickness inhomogeneities – less than 100 bar in oceanic lithosphere (BOTT & DEAN, 1972) – and stresses induced by (hypothetical) phase changes in the lithosphere under the influence of sediment loading (NEUGEBAUER & SPOHN, 1978).

For the reference model of sediment loading, the increase of the stresses generated as loading proceeds is compensated

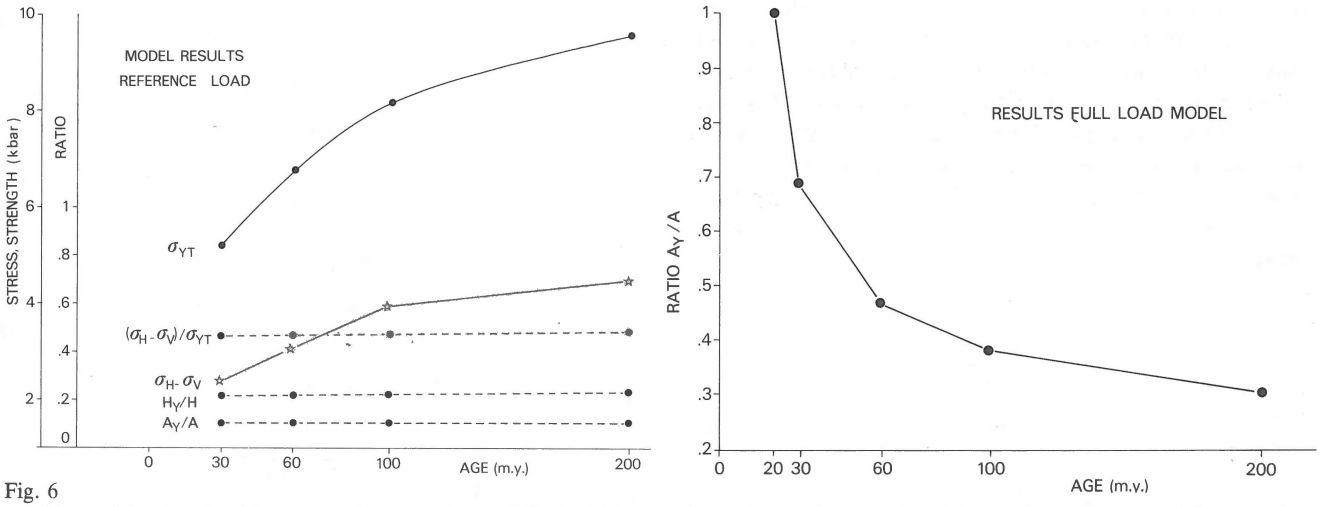

Fig. 6

a (left), Model results for the reference load: maximum differential stresses ($\sigma_H - \sigma_V$), tensile strength σ_{yT}, their ratio, the relative thickness of the mechanically strong upper part of the lithosphere in failure (H_y/H), and the ratio of A_y (the hatched area inside the strength envelope; see Fig. 5) and A (total area of the envelope) plotted as a function of lithospheric age. Stresses remain on a level too low to result in rupture of the lithosphere, no matter whether the margin is in a youthful or mature stage.

b (right), Results for the full load model: ratio of A_y and A as a function of lithospheric age. For ages below 20 m.y. lithospheric failure and consequently initiation of subduction is induced.

by a similar increase in the strength of the lithosphere. As a result the stresses at the passive margin for this sediment loading model will remain on a level too low to result in rupture of the lithosphere, no matter whether the margin is in a youthful or mature stage.

The situation changes however, when huge sedimentary masses (the full load model) are deposited on young (age below 20 m.y.) lithosphere. Under these circumstances stresses can be generated which are sufficiently high to induce lithospheric failure and initiation of subduction.

Owing to the stabilizing effect of the density changes accompanying the formation of oceanic crust (OXBURGH & PARMENTIER, 1977) oceanic lithosphere is gravitationally stable for ages less than 20-40 m.y. (WORTEL, 1980). As a result of its further cooling and thermal contraction the lithosphere becomes unstable for ages above 20-40 m.y. (OXBURGH & PARMENTIER, 1977; WORTEL, 1980). Taking into account only the gravitational instability of the lithosphere it was reasonable to expect that chances for initiation of subduction of oceanic lithosphere would increase with the age of the margin (VLAAR & WORTEL, 1976). The present work shows that if after a short evolution of the plate (time span a few tens of m.y.), subduction has not yet started, continued aging of the passive margin alone does not result in conditions more favourable for plate rupture and initiation of subduction.

From our results we may conclude that extensive sediment loading (following the full load model) might have been an effective mechanism for closure of young and presumably small ocean basins in geologic history.

Closing of small oceanic basins plays an important role in the process of mountain building. In this context it is interesting to note that studies of the Alpine orogeny show evidence for closing of oceanic basins in a relatively early stage after opening. For the Central Alps, FRISCH (1979) demonstrated closing of oceanic basins within the first 100 m.y. after opening. WINTERER & BOSELLINI (1981) have documented the evolution of a thickly sedimented Jurassic passive margin in the Southern Alps with closing of the oceanic basin approximately 50 m.y. after ocean floor spreading started.

For older margins in general it seems that the stresses generated by sediment loading are insufficient to induce lithospheric failure and initiation of subduction. Therefore, pre-existing weakness zones in oceanic lithosphere might be more suitable sites for initiation of subduction than passive margins. This view is consistent with the results of a survey of recently initiated subduction zones in the Pacific (KARIG, in prep.) showing that zones initiated in the Neogene are either at the sites of transform faults (as advocated earlier by UYEDA & BEN-AVRAHAM (1972)) or rejuvenated pre-existing subduction zones. Many of the present circum-Pacific zones are in fact the successors of subduction zones already present in the configuration prior to the break-up of Gondwanaland. Further back in geological time different plate configurations and a different thermal regime might have provided conditions more suitable for initiation of subducion. As an extreme example one might consider the Archaean where due to much steeper temperature profiles in the lithosphere (SHARPE & PELTIER, 1979), the oceanic lithosphere must have been considerably weaker than nowadays. In such a situation plate rupture requires a considerably lower stress level. This suggestion is corroborated by geological data on Precambrian orogenic belts (KRÖNER, 1981), showing extensive activation of passive margins bordering small oceanic basins.

In general, we expect initiation of subduction of oceanic lithosphere at passive margins not to play a primary role in

plate reorganizations such as documented by RONA & RICHARDSON (1978). However, in an oceanic plate attached to a subducting slab the pull acting on the downgoing lithosphere can be concentrated to a high level (order of magnitude several kilobars). In particular WORTEL & CLOETINGH (1981, 1982) have shown that lateral variations in the age of the slab descending in a subduction zone might provide a mechanism for fragmentation of oceanic plates, and the formation of spreading centres. Therefore, plate reorganization might take place predominantly by the formation of new spreading ridges.

ACKNOWLEDGEMENTS

We thank Prof. N. J. Vlaar for valuable discussions and Ir. Gerald Wisse (Scientific Applications Group of the Computing Centre, Delft University of Technology) for generous support with the finite element calculations.

REFERENCES

Bathe, K. J. & E. L. Wilson 1976 Numerical methods in Finite Element Analysis – Prentice-Hall Inc. (Englewood Cliffs N.J.): 528 pp.

Bodine, J. H., M.S. Steckler & A. B. Watts 1981 Observations of flexure and the rheology of oceanic lithosphere – J. Geophys. Res. 86: 3695-3707.

Bott, M. H. P. & D. S. Dean 1972 Stress systems at young continental margins – Nature Phys. Sci. 235: 23-25.

Bryant, W. R., R. H. Bennet & C. E. Katherman 1981 Shear strength, consolidation, porosity and permeability of oceanic sediments. In: C. Emiliani (ed.): The Sea 7 Wiley (New York: 1555-1616.

Buffler, R. T., F. J. Shaub, R. Huerta, A. B. Ibrahim & J. S. Watkins 1981 A model for the early evolution of the Gulf of Mexico basin – Oceanologica Acta: Coll. C3 Geology of continental margins. 26th Int. Geol. Congr. 1980 (Paris): 129-136.

Caldwell, J. G. & D. L. Turcotte 1979 Dependence of the thickness of the elastic oceanic lithosphere on age – J. Geophys. Res. 84: 7572-7576.

Chapple W.M. & D. W. Forsyth 1979 Earthquakes and bending of plates at trenches – J. Geophys. Res. 84: 6729-6749.

Cloetingh, S., G. Nolet & R. Wortel 1979 On the use of Rayleigh wave group velocities for the analysis of continental margins – Tectonophysics 59: 335-346.

—— 1980a Crustal structure of the eastern Mediterranean inferred from Rayleigh wave dispersion – Earth Planet. Sci. Lett. 51: 336-342.

—— 1980b Standard graphs and tables for the interpretation of Rayleigh wave group velocities in crustal studies – Kon. Ned. Akad. Wetensch. Proc., Ser. B. 83: 101-118.

Cloetingh, S. & G. Wisse 1981 Finite element modelling in Geodynamics: the state of stress at passive continental margins – Finite Element News 3: 37-40.

Cloetingh, S. A. P. L., M. J. R. Wortel & N. J. Vlaar 1981 On the State of stress at passive continental margins and the problem of initiation of subduction zones. 1980 EGS-ESC Mtg. (Budapest) Abstract – EOS Trans. Am. Geophys. Un. 62: 222.

—— 1982a State of stress at passive margins and initiation of subduction zones – Am. Assoc. Petrol. Geol. Mem. 34: in press.

—— 1982b Evolution of passive continental margins and initiation of subduction zones – Nature 297: 139-142.

Closs, H., H. Narain & S. C. Garde 1974 Continental margins of India. In: C. A. Burk & C. L. Drake (eds): The geology of continental margins – Springer (New York): 629-639.

Crough, S. T. 1975 Thermal model of oceanic lithosphere – Nature 256: 388-390.

Cromwell, J. C. 1974 Origin of late Cenozoic basins in southern California. In: W. R. Dickinson (ed.): Tectonics and sedimentation – Soc. Econ. Paleontol. Mineral. Spec. Publ. 22: 190-204.

Curray, J. R. & D. G. Moore 1974 Sedimentary and tectonic processes in the Bengal deep-sea fan and geosyncline. In C. A. Burk & C. L. Drake (eds.): The geology of continental margins – Springer (New York): 617-627.

Dewey, J. A. 1969 Continental margins: a model for conversion of Atlantic type to Andean type – Earth Plan. Sci. Lett. 6: 189-197.

Dickinson, W. R. & D. R. Seely 1979 Structure and Stratigraphy of forearc regions – Am. Assoc. Petrol Geol. Bull. 63: 2-31.

Dietz, R. S. 1963 Collapsing continental rises: an actualistic concept of geosynclines and mountain building – J. Geol. 7: 314-333.

Emery, K. O. 1980 Continental margins classification and petroleum prospects – Am. Assoc. Petrol. Geol. Bull. 64: 297-315.

Finetti, I & C. Morelli 1973 Geophysical exploration of the Mediterranea Sea – Boll. Geof. Teor. Appl. 15: 263-340.

Forsyth, D. W. & S. Uyeda 1975 On the relative importance of driving forces of plate motion – R. Astr. Soc. Geophys. J. 43: 163-200.

Frisch, W. 1979 Tectonic progradation and plate tectonic evolution of the Alps – Tectonophysics 60: 121-139.

Goetze, C. 1978 The mechanisms of creep in olivine – R. Soc. Lond. Phillos. Trans. Ser. A. 288: 99-119.

Goetze, C. & B. Evans 1979 Stress and temperature in the bending lithosphere as constrained by experimental rock mechanics – R. Astr. Soc. Geophys. J. 59: 463-478.

Goldflam, P., K. Hinz, W. Weigel & G. Wissmann 1980 Some features of the northwest African margin and magnetic quiet zone – R. Soc. Lond. Philos. Trans. Ser. A. 294: 87-96.

Grow, J. A., R. E. Mattick & J. S. Schlee 1979 Multichannel seismic depth sections and interval velocities over outer continental shelf and upper continental slope between Cape Hatteras and Cape Cod. In: J. S. Watkins, L. Montadert & P. W. Dickerson(eds): Geological and geophysical investigations of continental margins, Am. Assoc. Petrol. Geol. Mem. 29: 65-83.

Grow, J. A. & R. E. Sheridan 1981 Deep structure and evolution of the continental margin of the eastern United States – Oceanologica Acta. Coll. C3 Geology of continental margins. 26th Int. Geol. Congr. 1980 (Paris): 11-19.

Hales, A. L. 1969 Gravitational sliding and continental Drift – Earth Planet. Sci. Lett. 6: 31-34.

Haxby, W. F., D. L. Turcotte & J. M. Bird 1976 Thermal and mechanical evolution of the Michigan Basin – Tectonophysics 36: 57-75.

Hetényi, M. 1946 Beams on elastic foundation. Theory with applications in the fields of civil and mechanical engineering – University of Michigan Press (Ann Arbor, Michigan): 255 pp.

Hinz, K., H.U. Schlüter, A. C. Grant, S. P. Srivastava, D. Umpleby & J. Woodside 1979 Geophysical transects of the Labrador Sea: Labrador to Southwest Greenland – Tectonophysics 59: 151-183.

Houtz, R. E., W. J. Ludwig, J. D. Milliman & J. A. Grow 1977 Structure of the northern Brazilian continental margin – Geol. Soc. Am. Bull. 88: 711-719.

Hutchinson, D. R., J. A. Grow & K. D. Klitgord 1982 Deep structure and evolution of the Carolina trough. In: J. S. Watkins & C. L. Drake (eds): Continental margin processes – Am. Assoc.

Petrol. Geol. Mem. 34: in press.
Kanamori, H. 1980 Stress in the lithosphere. In: A. M. Dziewonski & E. Boschi (eds): Physics of the earth's interior – North Holland (Amsterdam): 712-713.
Keen, C. E. 1979 Thermal history and subsidence of rifted continental margins: Evidence from wells on the Nova Scotia and Labrador shelves – Can. J. Earth Sci. 16: 505-522.
Keen, C. E. & M. J. Keen 1974 Continental margins of eastern Canada and Baffin Bay. In: C. A. Burk & C. L. Drake (eds): The geology of continental margins – Springer (New York): 381-389.
Kent, P. E. 1974 Continental margin of East Africa, a region of vertical movement. In: C. A. Burk & C. L. Drake (eds): The geology of continental margins – (New York): 313-320.
Kirby, S. H. 1980 Tectonic stresses in the lithosphere: constraints provided by the experimental deformation of rocks – J. Geophys. Res. 85: 6353-6368.
Kröner, A. 1981 Precambrian plate tectonics. In: A. Kröner (ed.): Precambrian Plate Tectonics – Elsevier (Amsterdam): 57-90.
Lambeck, K. & S. M. Nakiboglu 1980 Seamount loading and stress in the ocean lithosphere – J. Geophys. Res. 85: 6403-6418.
Lehner, P. & P. A. C. De Ruiter 1977 Structural history of Atlantic margin of Africa – Am. Assoc. Petrol. Geol. Bull. 61: 961-981.
Malovitskiy, J. P., E. M. Emelyanov, O. V. Karakov, V. N. Moskalenko, G. V. Osipov, K. M. Shimkus & I. S. Chumakov 1975 Geological structure of the Mediterranean sea floor (based on geological-geophysical data) – Mar. Geol. 18: 231-261.
Marc Analysis Research Corporation 1980 Marc general purpose finite element program – User manual, A-E. (Palo Alto, California)
McAdoo, D. C., J. G. Caldwell & D. L. Turcotte 1978 On the elastic-perfectly plastic bending of the lithosphere under generalized loading with application to the Kuril Trench – R. Astr. Soc. Geophys. J. 54: 11-26.
McKenzie, D. P. 1967 Some remarks on heat-flow and gravity anomalies – J. Geophys. Res. 72: 6261-6273.
Minster, J. B. & D. L. Anderson 1980 Dislocations and non-elastic processes in the mantle – J. Geophys. Res. 85: 6347-6352.
Naini, B. R. 1980 A geological and geophysical study of the continental margin of Western India, and the adjoining Arabian Sea including the Indus Cone – Ph. D. Thesis, Colombia Univ. (New York) 172 pp.
Neugebauer, H. J. & T. Spohn 1978 Late stage development of mature Atlantic-type continental margins – Tectonophysics 50: 275-305.
Nolet, G., F. Panza & R. Wortel 1978 An averaged model for the Adriatic subplate – Pure and Appl. Geoph. 116: 1284-1298.
Oxburgh, E. R. & E. M. Parmentier 1977 Compositional and density stratification in oceanic lithosphere-causes and consequences – Geol. Soc. Lond. J. 133: 343-355.
Parsons, B. & J. G. Sclater 1977 An analysis of the variation of ocean floor heat flow and bathymetry with age – J. Geophys. Res. 82: 803-827.
Pollack, H. N. & D. S. Chapman 1977 On the regional variation of heat flow, geotherms and lithosphere thickness – Tectonophysics 38: 279-296.
Rona, P. A. & E. S. Richardson 1978 Early Cenozoic global plate reorganization – Earth Planet. Sci. Lett. 40: 1-11.
Sharpe, H. N. & W. R. Peltier 1979 A thermal history model for the Earth with parameterized convection – R. Astr. Soc. Geophys. J. 59: 171-203.
Steckler, M. S. & A. B. Watts 1981 Subsidence history and tectonic evolution of Atlantic type continental margins – Geodynamics Series 6, Am. Geophys. Un. (Washington D.C.): 184-196.
Stoneley, R. 1969 Sedimentary thicknesses in orogenic belts. In: P. E. Kent, et al. (eds): Time and place in orogeny – Geol. Soc. Lond.: 215-238.
Turcotte, D. L. & J. L. Ahern 1977 On the thermal and subsidence history of sedimentary basins – J. Geophys. Res. 82: 3762-3766.
Turcotte, D. L., J. L. Ahern & J. M. Bird 1977 The state of stress at continental margins – Tectonophysics 42: 1-28.
Turcotte, D. L. & E. R. Oxburgh 1967 Finite amplitude convective cells and continental drift – J. Fluid Mech. 28: 29-42.
Urien, C. M., L. R. Martins & J. J. Zambrano 1976 The geology and tectonic framework of southern Brazil, Uruguay and northern Argentina continental margin: their behaviour during the southern Atlantic opening. In: F. F. M. De Almeida (ed): Continental margins of Atlantic type – An. Acad. Bras. Cienc. 48 (suppl.): 365-376.
Uyeda, S. & Z. Ben-Avraham 1972 Origin and development of the Philippine sea: Nature 240: 176-178.
Vlaar, N. J. 1975 The driving mechanism of plate tectonics: a qualitative approach. In: G. J. Borradaile, A. R. Ritsema, H. E. Rondeel & O. J. Simon (eds): Progress in Geodynamics – North-Holland (Amsterdam): 234-245.
Vlaar, N.J. & M. J. R. Wortel 1976 Lithospheric aging, instability and subduction – Tectonophysics 32: 331-351.
Walcott, R. I. 1972 Gravity, flexure and the growth of sedimentary basins at a continental edge – Geol. Soc. Am. Bull. 83: 1845-1848.
Watkins, J. S. & C. L. Drake 1982 Continental margin processes – Am. Assoc. Petrol. Geol. Mem. 34: in press.
Watts, A. B., J. H. Bodine & M. S. Steckler 1980 Observations of flexure and the state of stress in the oceanic lithosphere – J. Geophys. Res. 85: 6369-6376.
Watts, A. B. & W. B. F. Ryan 1976 Flexure of the lithosphere and continental margin basins – Tectonophysics 36: 25-44.
Watts, A. B. & M. S. Steckler 1979 Subsidence and eustasy at the continental margin of eastern North America – Maurice Ewing Series 3, Am. Geophys. Un., (Washington D.C.): 218-234.
Winterer, E. L. & A. Bosellini 1981 Subsidence and sedimentation on Jurassic passive continental margin, Southern Alps, Italy – Am. Ass. Petrol. Geol. Bull. 65: 394-421.
Wortel, R. 1980 Age-dependent subduction of oceanic lithosphere – Ph. D. Thesis, Univ. of Utrecht (Utrecht) 147 pp.
Wortel, R. & S. Cloetingh 1981 On the Origin of the Cocos-Nazca spreading center – Geology 9: 425-430.
—— 1982 A mechanism for fragmentation of oceanic plates – Am. Ass. Petrol. Geol. Mem. 34: in press.
Zielinski, G. W. 1979 On the thermal evolution of passive continental margins, thermal depth anomalies and the Norwegian-Greenland Sea – J. Geophys. Res. 84: 7577-7588.
Zienkiewicz, O. C. 1977 The finite element method – McGraw-Hill (London) 787 pp.

APPENDIX

Finite element modelling in geodynamics

The finite element method allows the accurate calculation of stresses in an irregular inhomogeneous structure deformed by a system of distributed loads. In finite element analysis the structure is divided into a number of so-called finite elements, connected at nodal points. The displacements of the nodal points become the basic unknown quantities of the problem. This is the so-called displacement formulation. The state of displacement within each element as a function of the nodal displacements is now chosen. These functions also define the state of strain in the elements as a function of the nodal displacements. The strains in turn lead to the stresses within the element through a constitutive law. Finally a system of forces consistent with the modal displacements is found. These forces must be in equilibrium with the loads.

The geometrical and rheological properties of the structure are condensed in the stiffness matrix K. The displacements w of the structure, under a load F are found by solving the system:

$$[K]w = F \qquad \text{(A1)}$$

In linear elastic analysis the solution of the system is easily accomplished by triangularization of the matrix K in one single step. This is not possible in analysis of material non-linearity, like plasticity. Here small step, incremental approaches are needed. The two extreme procedures that may be followed in the solution of the non-linear equations are either a large number of small steps or one large step with many iterative cycles. In practice a combination of both is commonly used. In our analysis a mid-increment state is found for each integration point based on an incremental strain prediction. For the first cycle of each step this prediction is based on the strain increment of the preceding increment. At the start of each new increment, global equilibrium is enforced via the residual load correction. This prevents the accumulation of out of equilibrium forces from increment to increment.

For these reasons elastic-plastic finite element analysis requires considerably more computing time than the simple linear elastic calculations. The same applies for the computer memory needed to store the various parameters involved. Careful analysis is required to ensure convergence of the non-linear solution. In the present study up to 20 plastic increments were needed.

We have incorporated the depth-dependent strength profiles in the models by specifying yield strengths at the integration points of the elements, assuming linearity in the strength function between the integration points.

Having solved the equation A1 for the displacements, the calculation of the stresses σ follows straightforwardly. We illustrate this for the case of linear elasticity, were the procedure is as follows. First the strains e are calculated by e=[B]w, where B is the strain-displacement matrix. Subsequently stresses are found by using σ=[D]e = [D] [B]w, where D is the elasticity matrix. For non-linear analysis the procedure, although considerably more complicated, is based on this scheme (e.g. ZIENKIEWICZ, 1977; BATHE & WILSON, 1976).

The accuracy of the finite element computations is improved by increasing the number of elements and by selecting a higher interpolation order for the polynomial which describes the displacements of the element. Both steps imply a larger stiffness matrix for the problem, and as a result require more computer memory. An important advantage of taking an element with a higher order for the displacement function (a so-called higher order element) is that it allows the analysis to be carried out at the same accuracy, with a considerable reduction of the number of elements. In our work we have used eight node quadrilateral elements with a quadratic displacement function (linear strain). It can be easily shown that for accurate flexural analysis a quadratic displacement order is *required.* In the vertical direction we take five elements to discribe the linear stress distribution associated with bending.

The stress distribution in the horizontal direction is more complex than in the vertical direction. As a consequence in the first direction a relatively large number of elements is used, with a minimum length of the elements of 20 km. The models have a characteristic number of degrees of freedom of about 2000.

The deflection under the load is counteracted by isostasy. The classical one dimensional equation describing the flexure of a uniform elastic place under the influence of a load F with a hydrostatic restoring force is:

$$D\frac{d^4w}{dx^4} + (\varrho_m - \varrho_w)\, gw = F \qquad \text{(A2)}$$

where the hydrostatic restoring force $(\varrho_m - \varrho_w)$ is proportional to the deflection w and the density difference between the mantle (density ϱ_m) and the medium overlying the plate (usually water with density ϱ_w). D is the flexural rigidity of the plate, and g is the acceleration of gravity.

Equation A2 is equivalent to the linear system:

$$Kw + K^1w = F \qquad \text{(A3)}$$

where K is the operator $D\frac{d^4w}{dx^4}$ and K^1 equals $(\varrho_m - \varrho_w)$ g at the lower boundary of the plate and zero elsewhere. Translated into finite element language the operator $(K + K^1)$ is the stiffness matrix K_i, and the system A3 can now be written in the familiar form:

$$[K_i]w = F$$

where $K_i = K + K^1$ at the basal nodes of the plate, and $K_i = K$ elsewhere. Thus isostasy can be incorporated into the analysis by modifying the stiffness matrix at the basal nodes of the model. This is accomplished by the implementation of springs or an elastic foundation with a stiffness $(\varrho_m - \varrho_w)$ g in the model. In Fig. A1 we have plotted the finite element solution of eq.A2, for a triangular sedimentary load F on a uniform elastic infinite plate. We have adopted characteristics for the load and flexural properties for the plate corresponding to the reference load on uniform elastic 100 m.y. old lithosphere. Comparison of the resulting stresses and displacements with the analytical solution (HETÉNYI, 1946) of eq.A2 for this case shows that the finite element mesh is sufficiently fine for accurate

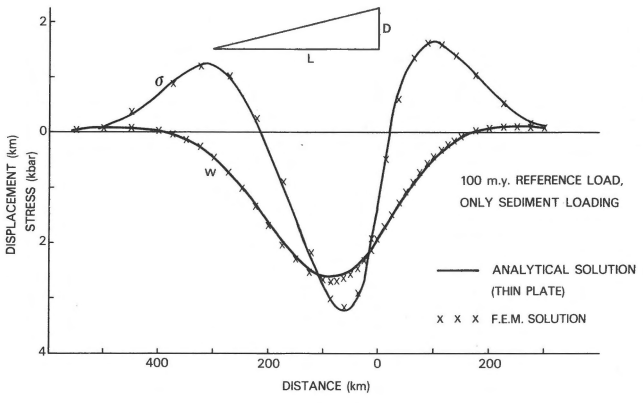

Fig. A1
The deflection of a uniform elastic infinite plate under the influence of a triangular load, counteracted by isotasy. Load characteristics (density, width L = 300 km, and height D) are for the reference model of sediment loading on 100 m.y. old lithosphere. Flexural properties are for a plate thickness of 44 km. Solid lines show the displacements (w) and maximum bending stresses (σ) according to the analytical test solution given by Hetényi (1946). Crosses (x) denote the displacements and stresses calculated with the finite element method.

analysis. It should be noted that finite element analysis is not hampered by the assumptions and limitations of classical thin plate theory encountered in methods of flexural analysis used by other workers (LAMBECK & NAKIBOGLU, 1980; BODINE ET AL., 1981). In particular the assumptions of a zero shear stress neutral surface and zero shear forces in the vertical plane are avoided. Thin plate theory overestimates the stiffness of the plate. Therefore, deflections are underestimated and bending stresses to a lesser extent, are, overestimated. Small deviations of the analytical solution from the finite element solution observed in Fig. A1 can be attributed to this effect. As a matter of fact, analytical test solutions are not available for the deformation of a plate with a depth-dependent non-linear elastic-plastic rheology under the influence of sediment loading and plate tectonic forces. Therefore, the accuracy of the model calculations presented in this paper was checked by convergence tests, made by refining the finite element meshes. An example of such a test is given in Fig. A2. A comparison of the results of two model calculations carried out with meshes differing by a factor two in the number of elements shows that the mesh spacing (mesh 1) used throughout the work guaranteed accurate analysis. Finally, the reaction forces of the model were checked to ensure equilibrium of external and internal forces.

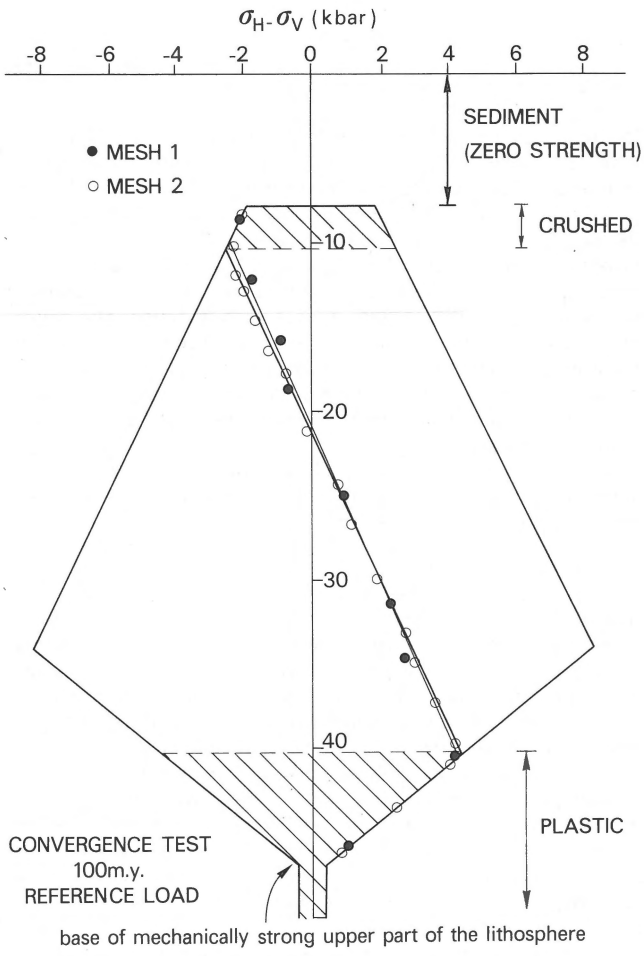

Fig. A2
Results of a convergence test on the 100 m.y. model used in the analysis (mesh 1). Geometrical and depth-dependent rheological properties vary across the margin and the reference model of sediment loading and plate tectonic forces are adopted. (see Fig. 3). Mesh 2 is the finite element mesh constructed by doubling the number of elements of mesh 1. Solid dots and open circles denote the results of the finite element stress calculations for mesh 1 and mesh 2 respectively. Their close correspondence confirms the accuracy of the model calculations.